Measurement of field-free alignment of jet-cooled molecules by nonresonant femtosecond degenerate four-wave mixing

Xiaoming Ren, Varun Makhija, and Vinod Kumarappan*
James R. Macdonald Laboratory, Kansas State University, Manhattan, Kansas 66506, USA
(Received 3 January 2012; published 5 March 2012)

A femtosecond degenerate four-wave mixing (fs-DFWM) technique for probing the alignment of molecules is described. The rotational wave packet generated by a strong pump beam modulates the nonresonant third-order susceptibility of the gas and this modulation is observed using a noncollinear background-free setup. As a demonstration of the technique, we measure the alignment of a linear molecule (nitrogen), a symmetric top (benzene), and an asymmetric top (iodobenzene) in a supersonic jet. The measured signal is shown to agree well with calculations of the nonresonant third-order susceptibility from the solution of the time-dependent Schrödinger equation. The pump-DFWM measurement scheme can be used with dilute jet-cooled targets, allows arbitrary pump pulses to be used, and is rapid enough to be incorporated into a feedback optimization loop. The scheme can easily be made polarization-sensitive, indicating the possibility of measuring and optimizing three-dimensional alignment of asymmetric-top molecules.

DOI: 10.1103/PhysRevA.85.033405 PACS number(s): 33.80.−b, 42.50.Hz, 33.15.Bh, 42.65.Re

I. INTRODUCTION

Gas-phase molecules can be aligned along laboratory axes using intense laser pulses [1]. Experiments in the adiabatic [2] and impulsive limits [3]—with laser pulses much longer and much shorter than the rotational period of the molecule, respectively—have shown that the nonresonant interaction of a molecule's polarizability with an intense laser pulse can confine the distribution of molecular axes in the laboratory frame. Alignment of gas-phase molecules has proven to be a powerful technique, leading to a range of applications, including high-harmonic generation from aligned molecules [4], molecular frame photoelectron spectroscopy [5], and laser-induced electron diffraction [6]. These and other potential applications such as ultrafast electron [7] and x-ray diffraction [8] have continued to drive interest in developing better methods for aligning molecules as well as for measuring the alignment under a range of experimental conditions. In this report we describe a versatile and general optical method for measuring the alignment of molecules that can be used even with dilute jet-cooled samples close to the nozzle and can potentially be extended to the measurement of three-dimensional alignment.

Advances in molecular alignment have been accompanied by the development of measurement techniques for characterizing the degree of alignment. The methods used can be broadly classified into fragment ion imaging methods (for example, see Refs. [2,3,9]) and optical methods (see Refs. [10–12]). The former yields detailed information about the angular distribution of the molecules but is limited in several ways. First, fragment ion imaging works only if the axial recoil approximation holds. If the fragment being measured is not ejected along the bond axis of the neutral molecule, the original angular distribution cannot be recovered. This limits the number of molecules that are amenable to these methods. Second, the efficiency of the fragmentation process depends on the orientation of the molecule with respect to the polarization of the laser pulse that induces the fragmentation [13]. The original angular distribution is, thus, convolved with this fragmentation efficiency which, for strong-field fragmentation in particular, is often not well understood. Even though clever choices of probe polarization directions [14,15] can sometimes circumvent this problem, this is a significant limitation. Finally, fragment imaging methods are unsuitable for dense targets, where space charge effects and the inability to operate a detector (a microchannel plate, for instance) can be prohibitive.

Optical methods are not limited by the same constraints. All molecular gases have linear and nonlinear susceptibilities in the laboratory frame that will change with molecular alignment. The relation between the molecular frame values of these susceptibilities and the laboratory frame values is easily determined—the two are connected by a rotation of the corresponding tensor. By measuring appropriate tensor components, moments of the angular distribution can be obtained. Since these susceptibilities are macroscopic quantities, it is necessary to have much higher target densities for optical measurement than are required for fragment imaging. But this requirement can be an advantage because these schemes allow the characterization of alignment in experiments such as high-harmonic generation [4] and filamentation [16] where high densities are essential. This is true for linear optical probes like optical birefringence [17] as well as for nonlinear ones like transient grating diffraction [18]. Here we describe a pump-probe experiment using fs-DFWM in a folded BOXCARS geometry, wherein three noncollinear input beams generate a four-wave mixing signal that is spatially separated from all the input beams by phase-matching conditions [19], as the probe. The technique is general, in that it can measure the alignment of a variety of molecules; it is also sensitive to the rotational motion of polyatomic molecules about all axes. The experimental details are discussed in Sec. II. In Sec. III, we describe our theoretical treatment of the probe and the calculation of the alignment signal by solving the time-dependent Schrödinger equation (TDSE). To demonstrate the effectiveness of this scheme, we describe in Secs. IV and

*vinod@phys.ksu.edu

V the alignment of nitrogen molecules in a neat supersonic expansion and that of benzene and iodobenzene molecules seeded in a high-pressure helium jet. The ability to use a dilute sample seeded in helium is very advantageous in alignment experiments due to the low rotational temperatures that can be achieved [20].

II. NONRESONANT DFWM AS A PROBE OF ALIGNMENT

The experimental setup is shown in Fig. 1. Laser pulses from the Kansas Light Source, a multipass amplified Ti:sapphire laser (2-kHz, 2-mJ/pulse, 790-nm central wavelength, 30-fs pulse duration, 1-cm beam size), are split into pump and probe arms on a broadband 50:50 dielectric beam splitter. The pump pulse is telescoped down to 6 mm; passes through a 6-mm hole in a 2-inch, 45° dielectric mirror; and is focused by a 2-inch diameter, 35-cm focal length lens (L1) into a vacuum chamber. The probe beam is delayed by a 30-cm-long motorized delay stage and then expanded by a telescope to 50-mm diameter. This beam is recombined with the pump on the 2-inch mirror-with-a-hole, after which it passes through a 50 × 50 mm aluminum plate with three 8-mm-diameter holes at the corners of a 10-mm square. A 6-mm hole at the center of the square also lets the pump beam through. The probe beam is also focused into the vacuum chamber by the same lens. Spatial and temporal overlap between the three probe beams is, thus, automatically obtained and is almost jitter free.

At the focus, the pump and probe beams interact with a gas pulse produced by a kHz Even-Lavie valve [21]. Nitrogen gas was cooled in a neat expansion. When using liquid samples, the valve is operated with 70 bar of helium and a small amount of the liquid (benzene and iodobenzene in our case) is placed inside the body of the valve so the sample can be entrained in the supersonic expansion from the nozzle. Although we have not made any direct measurements in our own experiment, the Even-Lavie valve can cool iodobenzene molecules to a rotational temperature of ∼1 K [20]. In the absence of the pump beam, the three probe beams interact nonlinearly with the target molecules to produce a four-wave mixing signal. In this widely used geometry the DFWM signal is automatically phase matched along the direction of the unoccupied corner of the square. The signal is, thus, coherent and noncollinear with all the input beams, including the pump. This feature allows background-free detection. In order to remove almost all the scattered light from the signal beam before it strikes a detector, lenses L1 and L2 image the first square onto an image plane after the vacuum chamber, where an iris at the position of the expected signal beam lets only the signal beam to pass through. The telescope formed by lenses L2 and L3 images the pump focus onto a 50-μm pinhole placed immediately before the avalanche photodiode detector. This confocal detection geometry not only improves the signal-to-noise ratio but also restricts the region of space in the interaction region from which the signal is detected. This allows us to monitor signal only from the central portion of the pump beam where the highest degree of alignment is obtained. The detrimental effects of focal-volume averaging are, thus, minimized; in Secs. IV and V we will show that TDSE calculations that do not include intensity averaging agree well with experimental data.

When the probe pulse arrives before the pump pulse, it encounters an isotropic medium. The DFWM signal measured in this case depends on the molecular susceptibility tensor, the intensity of the probe pulses, and the density of gas. In our setup, the three pulses are always overlapped in time and the signal we measure is usually known as the coherent artifact in DFWM measurements. When ultrashort pulses are used, the coherent artifact is dominated by the nonresonant part of the susceptibility even when there are vibrational resonances

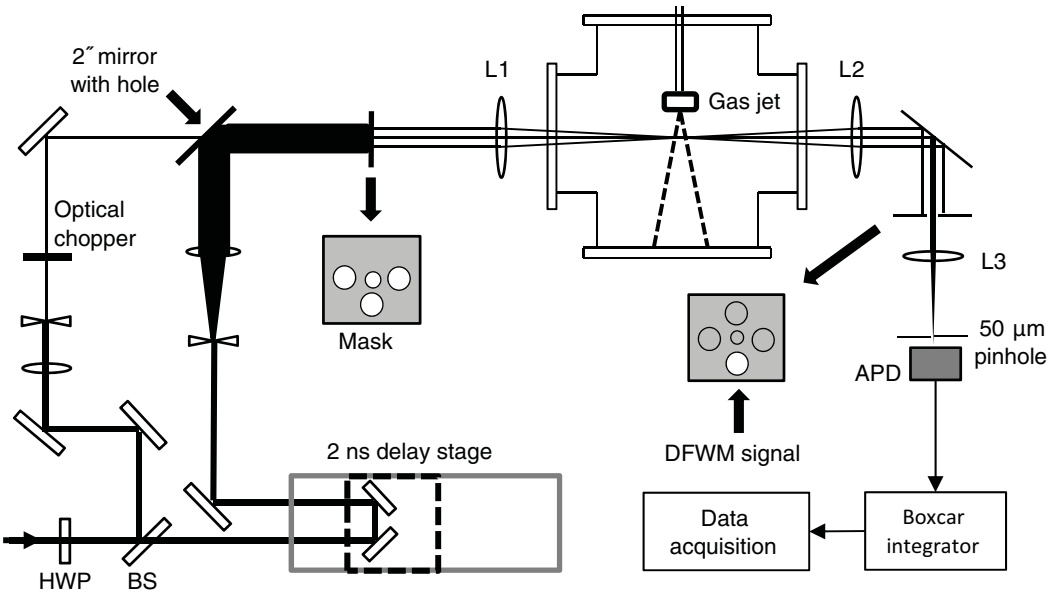

FIG. 1. Schematic diagram of the pump-DFWM setup. Pump and probe beams are overlapped on the 2-inch mirror, which has a 6-mm hole, the single probe beam is split into three beams using an aluminum mask, all the beams are focused in the jet by lens L1, and the DFWM signal is spatially filtered using a telescope (lenses L2 and L3) and a pinhole in front of an avalanche photodiode (APD).

within the bandwidth of the laser [22]. The measured DFWM signal can be used to normalize the alignment measurement. We implement the normalization and a correlated double sampling scheme by operating the laser at 2 kHz and the gas jet at 1 kHz and by chopping the pump beam at 500 Hz. This chopping scheme produces four distinct combinations of gas and pump beams (the probe is always present): (a) gas and pump are both on; (b) the gas is off but pump is on; (c) the gas is back on, but the pump is blocked by the chopper; and (d) both gas and pump are off. Thus, we have four types of signal corresponding to these combinations: (a) full signal including scattered light from pump and probe, (b) only scattered light from pump and probe, (c) signal and scattered light from the probe alone, and (d) scattered light from the probe alone. The signal from the detector is boxcar integrated shot by shot and acquired by a computer, which also acquires digital signals indicating whether the gas jet and/or the pump beam are on. Simple algebra carried out on the computer removes the scattered light signal and normalizes the pump-probe signal with respect to the probe-only signal. Thus, the average number of molecules in the laser focus, the volume of the focus, and the intensity of the probe beams are all factored out and this scheme provides a calibrated measurement of the third-order susceptibility of the target. The sources of noise that remain are shot-to-shot fluctuations in laser energy and the number density in the gas jet; the data shown below were averaged over up to 1000 cycles of four laser shots each to overcome these.

Noncollinear fs-DFWM has several advantages over other schemes that have been used so far to characterize alignment. First, it is versatile in that the pump (which can be a sequence of pulses) can have arbitrary shape and polarization. This is not the case in DFWM measurements using two strong pulses to set up an alignment grating—the asymmetric top alignment grating that will be set up by two cross-polarized pulses would already be quite complex. Second, since the probe is both perturbative and nonresonant, the interpretation of the signal is relatively straightforward. Third, with a coherent noncollinear process the target density required is quite low. We show evidence of this in Sec. V, where we discuss alignment of low-density iodobenzene seeded in helium. Fourth, this method raises the prospect of measuring impulsive 3D alignment with any suitable pump pulses. Since several polarization configurations can easily be obtained by inserting wave plates in the probe beams and a polarizer in the signal beam, the corresponding tensor susceptibility components can be measured and 3D alignment could potentially be inferred. This method suffers from neither the ambiguity of velocity map imaging measurements [15], which do not provide any useful information unless the 3D alignment is already quite good, nor the long measurement time required for multi-ion coincidence measurements [14].

III. CALCULATION OF ROTATIONAL DYNAMICS AND DFWM SIGNAL

We calculate the rotational dynamics of molecules using the polarizability interaction assuming no vibronic excitation from the ground state. The Hamiltonian is

$$H = H_{\rm rot} - \tfrac{1}{4}\mathbf{E}(t)\cdot[\boldsymbol{\alpha}\mathbf{E}(t)], \qquad (1)$$

where the polarizability tensor $\boldsymbol{\alpha}$ and the field-free Hamiltonian $H_{\rm rot}$ vary depending on the complexity of the molecules [23] and $\mathbf{E}(t)$ is the envelope of the laser electric field. The rotational wave packet is obtained by solving the TDSE for this Hamiltonian for a thermal distribution of initial states, including nuclear spin statistics (for a review of the theory of intense laser alignment, see Ref. [24]). The calculations are carried out for a single peak intensity; focal volume averaging is not included. The expectation values of the susceptibility components are then calculated from the propagated wave function, with the assumption that the 30-fs probe pulses are sufficiently short that rotational dynamics during the probe pulse duration can be ignored. Since the experimental setup measures the ratio of the time-dependent DFWM signal to the isotropic value under identical conditions, other variables, including the number density of the target gas and the probe intensities, are automatically factored out and need not be taken into account.

In order to calculate the expectation values of the susceptibility components we need the molecular frame hyperpolarizability tensor components. The unique nonzero elements for the molecules studied in this article were obtained from Ref. [25] (for benzene and iodobenzene) and Ref. [26] (for nitrogen). The point group symmetry of the molecule, the symmetry of electronic ground state, and the degeneracy of photon frequencies add further nonzero tensor elements. These are tabulated in Ref. [27].

To derive an expression for the third-order susceptibility tensor components for linear and symmetric tops, the molecular frame second hyperpolarizability tensor is rotated to the laboratory frame. The unique nonzero components of the second hyperpolarizability in the ground vibronic state are γ_{zzzz}, γ_{xxxx}, and γ_{xxzz} for linear molecules and γ_{zzzz}, γ_{xxxx}, γ_{xxzz}, and γ_{xxyy} for symmetric tops, where z is the molecular symmetry axis. The symmetry of linear and symmetric tops allows x and y to be interchanged, and the degeneracy of the frequencies in DFWM allows all four indices of the tensor to be permuted, adding 12 additional components for linear molecules and 14 for symmetric tops. Rotating this tensor to the laboratory frame gives the required susceptibility component,

$$\chi^{(3)}_{ijkl} = N\epsilon_0\langle R_{im}R_{jn}R_{ko}R_{lp}\rangle\gamma_{mnop}, \qquad (2)$$

where the R_{ij} are elements of the rotation matrix that transforms the molecular frame to the laboratory frame, N is the number density of molecules, and the expression is summed over repeated indices.

After the interaction with the pump pulse, which is linearly polarized along the laboratory frame Z axis, the ensemble averages of the susceptibility tensor components do not depend on the Euler angles χ and ϕ for both linear and symmetric top molecules. The remaining expressions contains only the moments of $\cos\theta$ and are easily evaluated from Eq. (2). However, this is not true for asymmetric top molecules, where the polarizability interaction with the laser pulse involves the angle χ [24]. Equation (2) is too cumbersome in that case, and in order to calculate third-order susceptibility components of asymmetric top molecules we derive an expression for the matrix elements of the components in the symmetric top basis

$|JKM\rangle$, where J is the total angular momentum and K and M are the projections along the z axis (the molecular symmetry axis) and the Z axis (the polarization of the pump pulse), respectively. We start by rewriting the Cartesian molecular hyperpolarizability tensor in the spherical basis by extending the procedure described in Ref. [23] (p. 216) for second-rank tensors. For iodobenzene the unique nonzero Cartesian tensor components are γ_{zzzz}, γ_{xxxx}, γ_{yyyy}, γ_{xxzz}, γ_{xxyy}, and γ_{yyzz}. Taking into account the degenerate field frequencies as before adds 15 more components. In the spherical basis the tensor rotates to the laboratory frame via the Wigner matrices, and

$$\chi^l_m = N\epsilon_0 \sum_{m'} D^l_{m',m}\gamma^l_{m'}, \tag{3}$$

where χ^l_m and $\gamma^l_{m'}$ are spherical components of the susceptibility and hyperpolarizability tensors, respectively, and $D^l_{m',m}$ are the Wigner matrices. For third-rank tensors, $l = 0,1,2,3$ or 4 and $m = -l,-l+1,\ldots,l-1,l$. Since the $|JKM\rangle$ functions are proportional to the Hermitian conjugates of the Wigner matrices [23], the matrix elements $\langle JKM|\chi^l_m|J'K'M'\rangle$ are easily obtained in terms of Clebsch-Gordan coefficients ([23], p. 102). Transforming these back to the Cartesian basis gives the matrix elements for the required Cartesian susceptibility component in the $|JKM\rangle$ basis. For asymmetric tops the Schrödinger equation is also solved in the symmetric top basis as described in Ref. [8]. The expectation values of the susceptibility components are then calculated from the propagated wave function using the derived matrix elements.

IV. RESULTS: LINEAR AND SYMMETRIC TOP MOLECULES

Alignment of linear molecules has been studied experimentally by use of a wide variety of methods, including optical birefringence [10], transient gratings [11], spectral interferometry [12], and Coulomb explosion imaging [3,9]. In Fig. 2(a), we show the measurement of the degree of alignment of N_2 molecules using the pump-DFWM scheme, as well as the results of the TDSE calculation of the normalized signal. The $ZZZZ$ component of the DFWM signal, where Z is the axis of polarization of the pump, was measured. The signal is normalized with respect to the isotropic value of the susceptibility. Note that, as a result of measuring the square of the susceptibility, we access eighth-order moments of the distribution, allowing the measurement of weak one-eighth revivals. For this component, the normalized signal for perfect alignment along the Z axis is calculated to be 1.99. In the experimental data, we can see that the maximum alignment is 1.28, based on the TDSE calculation $\langle\cos^2\theta\rangle = 0.53$ (the isotropic value is $1/3$). Note that the calculated time-dependent susceptibility component and the $\langle\cos^2\theta\rangle$ traces seem to be identical; the reason can be clearly seen in the expression for the normalized susceptibility χ^2_{ZZZZ} in terms of the Wigner matrix elements. This expression has the form

$$\chi^2_{ZZZZ}(t) = \sum_{J=0}^{4} C_J D^{2J}_{00}(\theta,\phi,\chi), \tag{4}$$

where the coefficients are $C_0 = 1$, $C_2 = 1.016$, $C_4 = 0.00587$, $C_6 = 0.026$, and $C_8 = 0.00136$. The $D^2_{00} = (3\cos^2\theta - 1)/2$ term is dominant over other terms. In this case, the value of $\langle\cos^2\theta\rangle$ can be read off the experimental trace directly. For larger molecules benzene and iodobenzene, the higher-order terms are more important and will become apparent in the time evolution of the susceptibility, but the $\langle\cos^2\theta\rangle$ remains the dominant contributor to the $ZZZZ$ component.

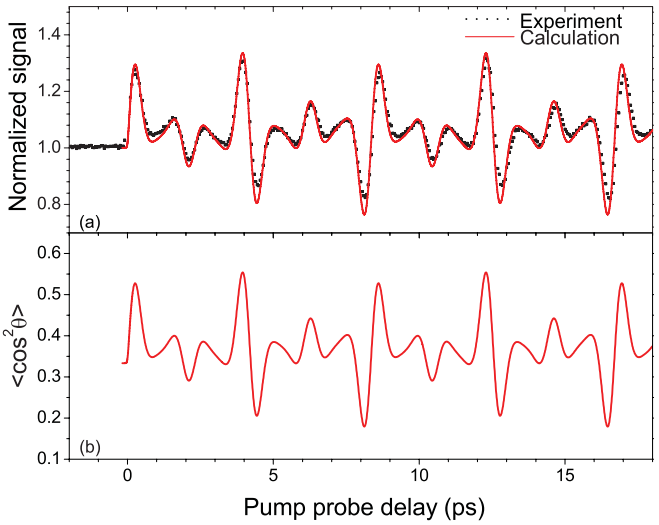

FIG. 2. (Color online) (a) Pump-DFWM measurement of alignment of nitrogen. The supersonic jet was operated with 70 bar of nitrogen. Black scatter plot is experimental data; the pump pulse had 30 TW/cm^2 peak intensity and 60 fs FWHM. The calculation (solid red line) was carried out at a rotational temperature of 20 K to get best agreement with the experiment, the pump pulse was 30 TW/cm^2 and 60 fs FWHM. There are no other free parameters in the calculation. (b) The evolution of $\langle\cos^2\theta\rangle(t)$ from the same calculation.

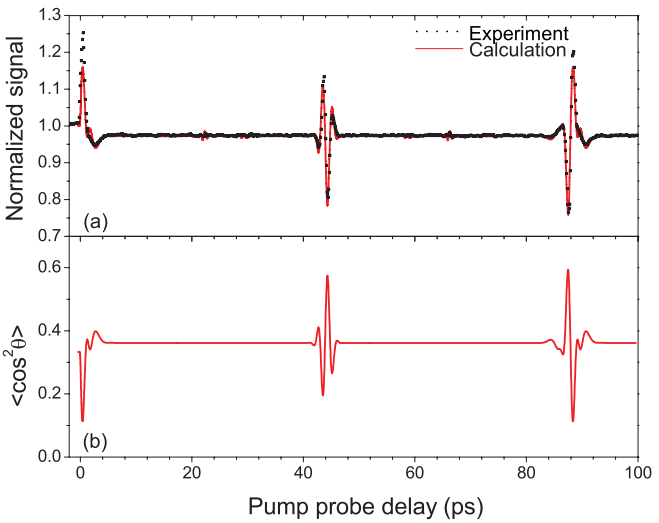

FIG. 3. (Color online) (a) Pump-DWFM measurement of the alignment of benzene. The supersonic jet was operated with 70 bar backing pressure of helium. In the experiment (black scatter plot), the pump pulse was 15 TW/cm^2 and 130 fs FWHM. The calculation (solid red line) of alignment was carried out at 35 K to get best agreement with the experiments, pump pulse was 15 TW/cm^2 and 130 fs FWHM. There are no other free parameters in the calculation. (b) The evolution of $\langle\cos^2\theta\rangle(t)$ from the same calculation.

Figure 3 shows the measured and calculated revival spectra for benzene molecules seeded in 70 bar of helium. The vapor pressure of benzene at 50 °C is ∼360 mbar. Benzene is an oblate symmetric top and its symmetry axis (perpendicular to the plane of the ring) is also its least polarizable axis. The linearly polarized pump pulse drives the least polarizable axis of the molecule away from the polarization vector, creating a distribution that is initially antialigned. Thus, $\langle\cos^2\theta\rangle$, defined as the angle between the Z axis and the C_6 axis of benzene, initially falls below its isotropic value of $1/3$. After the wave-packet components have dephased, the baseline is greater than $1/3$ due to incoherent or population alignment that results when $\langle J^2\rangle \gg \langle M^2\rangle$ [28]. Unlike a linear molecule where incoherent alignment results in (weak) alignment of the molecular axis with the laser polarization, in this case incoherent alignment leads to planar alignment—the molecular plane is weakly confined to the plane perpendicular to the pump polarization. This feature can be seen in the experimental trace in the form of a downward shift of the baseline after the initial alignment peak, in agreement with the calculation.

The calculated trace for the DFWM signal shows strong revivals at the full and half-revival periods and significantly weaker revivals at one-third, one-fourth, and one-eighth of the full revival time. The experimental trace agrees well with calculated trace, although some expected revivals are too small in magnitude to be seen. In this trace, the calculated maximum $\langle\cos^2\theta\rangle$ value is 0.59 at the first full revival. The minimum value is 0.11 during the initial alignment peak. This value corresponds to a strong localization of the symmetry axis of benzene to the XY plane.

V. RESULTS: ASYMMETRIC TOP MOLECULES

We align iodobenzene, which has been studied extensively in the context of molecular alignment using velocity map imaging, to demonstrate the strengths of confocal fs pump-DFWM as a tool for characterizing molecular alignment. A small quantity of liquid iodobenzene (vapor pressure ∼18 mbar at 70 °C) is placed inside the body of the Even-Lavie valve and the molecules are carried by the high-pressure helium as it expands through the nozzle. After adiabatic expansion, rotational temperatures below 1 K can be achieved in this configuration, although we have not measured it directly. Moreover, the interaction region is within a few mm of the nozzle, and we do not expect the cooling process to be complete. The target likely to be somewhat warmer than the ultimate sub-Kelvin temperature.

Figure 4 shows a measurement of the time evolution of the normalized signal in the $ZZZZ$ configuration after the molecules were hit by a 60-fs, 18-TW/cm^2 pulse. J- and C-type revivals that result from the rephasing of $\Delta J = \pm 1, \pm 2$, $\Delta K = 0$ and $\Delta J = \pm 2, \Delta K = 0$ coherences [29], respectively, can be seen in the experimental data. The agreement between the experiment and calculation is good—except for some of the details shown in the inset in Fig. 4. A more careful comparison would require better signal-to-noise ratio and temperature in the measurement and possibly better values for the hyperpolarizability tensor of iodobenzene. The calculation also ignores volume averaging,

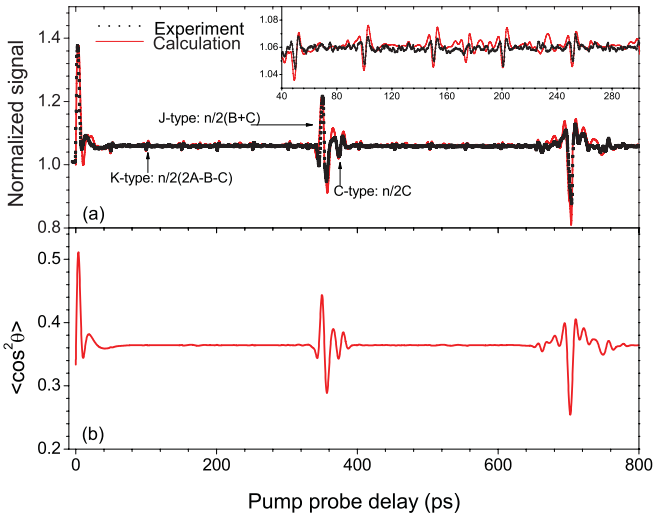

FIG. 4. (Color online) (a) Alignment revivals in iodobenzene. The $ZZZZ$ components from both experiment (black scatter plot) and calculation (solid red line) are shown. Since the signal depends on Euler angles θ and χ, weak K-type revivals are seen. In experiment the pump pulse had 18 TW/cm^2 peak intensity and 60 fs FWHM. The calculation of alignment was carried out at 8 K to get best agreement with the experiments; pump pulse was 15 TW/cm^2 and 60 fs. (b) The evolution of $\langle\cos^2\theta\rangle(t)$ from the same calculation.

centrifugal distortion of the molecules, and any strong field effects in the DFWM process [30,31]. Based on the calculation, the maximum $\langle\cos^2\theta\rangle$ value is 0.51 for the initial alignment peak. Each data point is averaged over 1000 cycles of four laser shots each. After including the overhead for the computer and translation stage, the average time per point is about 4 s. A genetic algorithm with population of 30 individuals running for 50 generations will take less than 2 h—a reasonable amount of time for such optimization.

Since the interaction Hamiltonian for the pump pulse and the signal depend on the angle χ in this polarization geometry, revivals in rotation about the molecular C-I axis are expected. The K-type revivals [29] can be seen in Fig. 4 at the expected times, $T_{\rm rev} = n/(4A - 2B - 2C)$. Since iodobenzene is a nearly prolate molecule ($A = 5.672$ GHz, $B = 0.75$ GHz, $C = 0.663$ GHz), these revivals are quite regular, although not strictly periodic. K-type revivals can, in principle,[1] be seen in a $\langle\cos^2\theta\rangle$ measurement from the momentum distribution of the I^+ fragment, but, in practice, the expected revivals are very small and would be hard to measure. The DFWM measurement is sensitive to rotations about all the three axes in asymmetric top molecules, which indicates that it should be capable of measuring 3D alignment.

VI. SUMMARY

By adapting degenerate four-wave mixing and a simple folded-BOXCARS geometry, we have developed a versatile

[1]Very weak K-type revivals ($\Delta K = \pm 2$) appear in $\langle\cos^2\theta\rangle$ ($\Delta K = 0$) because the laser pulse excites a broad wave packet in both J and K, and $\langle\cos^2\theta\rangle$ includes the interference of the contributions from many values of K.

scheme for rapid optical characterization of molecular alignment in cold and relatively sparse gas targets. The most important advantage of this method is the separation of the pump and probe processes. By using a perturbative probe that does not depend on the pump pulse, it is possible to use arbitrarily shaped pulses in the pump-DFWM scheme. For instance, sequences of orthogonally polarized pulses and even polarization-shaped pulses can be used. Computationally, we have shown that this scheme, which imposes a nonlinear but perturbative modulation on a very broad wave packet resulting from a highly nonperturbative excitation, provides a well-calibrated measurement of alignment. The agreement between experiment and the theory will likely improve if focal volume averaging, centrifugal distortion, and strong field corrections to the DFWM process are included.

With the addition of half-wave plates in the probe beam and a polarizer in the signal beam, polarization-resolved measurements of the target susceptibility tensor are possible. We expect to be able to characterize 3D alignment with a suitable choice of components to measure. These experiments are in progress. Since the signal can be measured with good signal-to-noise ratio in a few seconds even for very dilute targets, this measurement scheme is easily incorporated into a feedback-optimization loop with a pulse shaper to take advantage of the low rotational temperatures. We have shown that this method can be used with pure gases at high density and with seeded samples with less than a mTorr of partial pressure. This technique should prove useful for characterizing the alignment of polyatomic molecules for high-harmonic generation and x-ray diffraction experiments.

ACKNOWLEDGMENTS

This work was supported by the Chemical Sciences, Geosciences, and Biosciences Division, Office of Basic Energy Sciences, Office of Science, US Department of Energy.

[1] H. Stapelfeldt and T. Seideman, Rev. Mod. Phys. **75**, 543 (2003).
[2] H. Sakai, C. P. Safvan, J. J. Larsen, K. M. Hilligsoe, K. Hald, and H. Stapelfeldt, J. Chem. Phys. **110**, 10235 (1999).
[3] F. Rosca-Pruna and M. J. J. Vrakking, Phys. Rev. Lett. **87**, 153902 (2001).
[4] R. Velotta, N. Hay, M. B. Mason, M. Castillejo, and J. P. Marangos, Phys. Rev. Lett. **87**, 183901 (2001).
[5] V. Kumarappan, L. Holmegaard, C. Martiny, C. B. Madsen, T. K. Kjeldsen, S. S. Viftrup, L. B. Madsen, and H. Stapelfeldt, Phys. Rev. Lett. **100**, 093006 (2008).
[6] M. Meckel, D. Comtois, D. Zeidler, A. Staudte, D. Pavičić, H. C. Bandulet, H. Pépin, J. C. Kieffer, R. Dörner, D. M. Villeneuve, and P. B. Corkum, Science **320**, 1478 (2008).
[7] P. Reckenthaeler, M. Centurion, W. Fuß, S. A. Trushin, F. Krausz, and E. E. Fill, Phys. Rev. Lett. **102**, 213001 (2009).
[8] S. Pabst, P. J. Ho, and R. Santra, Phys. Rev. A **81**, 043425 (2010).
[9] P. W. Dooley, I. V. Litvinyuk, K. F. Lee, D. M. Rayner, M. Spanner, D. M. Villeneuve, and P. B. Corkum, Phys. Rev. A **68**, 023406 (2003).
[10] V. Renard, M. Renard, S. Guerin, Y. T. Pashayan, B. Lavorel, O. Faucher, and H. R. Jauslin, Phys. Rev. Lett. **90**, 153601 (2003).
[11] A. Rouzee, V. Renard, S. Guerin, O. Faucher, and B. Lavorel, Phys. Rev. A **75**, 013419 (2007).
[12] Y. H. Chen, S. Varma, A. York, and H. M. Milchberg, Opt. Express **15**, 11341 (2007).
[13] I. V. Litvinyuk, K. F. Lee, P. W. Dooley, D. M. Rayner, D. M. Villeneuve, and P. B. Corkum, Phys. Rev. Lett. **90**, 233003 (2003).
[14] K. F. Lee, D. M. Villeneuve, P. B. Corkum, A. Stolow, and J. G. Underwood, Phys. Rev. Lett. **97**, 173001 (2006).
[15] S. S. Viftrup, V. Kumarappan, S. Trippel, H. Stapelfeldt, E. Hamilton, and T. Seideman, Phys. Rev. Lett. **99**, 143602 (2007).
[16] S. Varma, Y.-H. Chen, and H. M. Milchberg, Phys. Rev. Lett. **101**, 205001 (2008).
[17] V. Renard, M. Renard, A. Rouzee, S. Guerin, H. R. Jauslin, B. Lavorel, and O. Faucher, Phys. Rev. A **70**, 033420 (2004).
[18] M. Comstock, V. Senekerimyan, and M. Dantus, J. Phys. Chem. A **107**, 8271 (2003).
[19] J. A. Shirley, R. J. Hall, and A. C. Eckbreth, Opt. Lett. **5**, 380 (1980).
[20] V. Kumarappan, C. Z. Bisgaard, S. S. Viftrup, L. Holmegaard, and H. Stapelfeldt, J. Chem. Phys. **125**, 194309 (2006).
[21] U. Even, J. Jortner, D. Noy, N. Lavie, and C. Cossart-Magos, J. Chem. Phys. **112**, 8068 (2000).
[22] J.-x. Cheng, A. Volkmer, L. D. Book, and X. S. Xie, J. Phys. Chem. B **105**, 1277 (2001).
[23] R. N. Zare, *Angular Momentum: Understanding Spatial Aspects in Chemistry and Physics* (Wiley-Interscience, New York, 1988).
[24] T. Seideman and E. Hamilton, *Nonadiabatic Alignment by Intense Pulses: Concepts, Theory, and Directions*, in Advances in Atomic Molecular and Optical Physics, Vol. 52, edited by P. R. Berman and C. C. Lin (Elsevier Academic Press, Amsterdam, 2005), pp. 289–329.
[25] N. Matsuzawa and D. A. Dixon, J. Phys. Chem. **98**, 2545 (1994).
[26] G. Maroulis and D. Bishop, Mol. Phys. **58**, 273 (1986).
[27] R. P. Davis, A. J. Moad, G. S. Goeken, R. D. Wampler, and G. J. Simpson, J. Phys. Chem. B **112**, 5834 (2008).
[28] T. Seideman, Phys. Rev. Lett. **83**, 4971 (1999).
[29] P. W. Joireman, L. L. Connell, S. M. Ohline, and P. M. Felker, J. Chem. Phys. **96**, 4118 (1992).
[30] V. G. Stavros, E. Harel, and S. R. Leone, J. Chem. Phys. **122**, 064301 (2005).
[31] M. F. Gelin, C. Riehn, M. Kunitski, and B. Brutschy, J. Chem. Phys. **132**, 134301 (2010).